BMJ Open Ophthalmology

In vivo crystalline lens measurements with novel swept-source optical coherent tomography: an investigation on variability of measurement

Takuhei Shoji, Naoko Kato, Sho Ishikawa, Hisashi Ibuki, Norihiro Yamada, Itaru Kimura, Kei Shinoda

To cite: Shoji T, Kato N, Ishikawa S, *et al*. In vivo crystalline lens measurements with novel swept-source optical coherent tomography: an investigation on variability of measurement. *BMJ Open Ophth* 2017;**1**:e000058. doi:10.1136/bmjophth-2016-000058

Received 22 November 2016
Revised 20 January 2017
Accepted 12 February 2017

Department of Ophthalmology, Saitama Medical University, Iruma, Saitama, Japan

Correspondence to
Dr Takuhei Shoji; shoojii@gmail.com

ABSTRACT

Objective: To evaluate the reproducibility of in vivo crystalline lens measurements obtained by novel commercially available swept-source (SS) optical coherence tomography (OCT) specifically designed for anterior segment imaging.

Methods and analysis: One eye from each of 30 healthy subjects was randomly selected using the CASIA2 (Tomey, Nagoya, Japan) in two separate visits within a week. Each eye was imaged twice. After image scanning, the anterior and posterior lens curvatures and lens thickness were calculated automatically by the CASIA2 built-in program at 0 dioptre (D) (static), −1 D, −3 D and −5 D accommodative stress. The intraobserver and intervisit reproducibility coefficient (RC) and intraclass correlation coefficient (ICC) were calculated.

Results: The intraobserver and intervisit RCs ranged from 0.824 to 1.254 mm and 0.789 to 0.911 mm for anterior lens curvature, from 0.276 to 0.299 mm and 0.221 to 0.270 mm for posterior lens curvature and from 0.065 to 0.094 mm and 0.054 to 0.132 mm for lens thickness, respectively. The intraobserver and intervisit ICCs ranged from 0.831 to 0.865 and 0.828 to 0.914 for anterior lens curvature, from 0.832 to 0.898 and 0.840 to 0.933 for posterior lens curvature and from 0.980 to 0.992 and 0.942 to 0.995 for lens thickness. High ICC values were observed for each measurement regardless of accommodative stress. RCs in younger subjects tended to be larger than those in older subjects.

Conclusions: This novel anterior segment SS-OCT instrument produced reliable in vivo crystalline lens measurement with good repeatability and reproducibility regardless of accommodation stress.

Key messages

What is already known about this subject?

- Though optical coherence tomography (OCT) is increasingly used for in vivo crystalline lens analysis, custom-made OCT is needed to study biometry analysis during accommodation in vivo and in real time.

What are the new findings?

- Novel commercially available swept-source OCT specifically designed for anterior segment imaging can measure whole lens image and calculate anterior and posterior curvatures and lens thickness automatically with good repeatability and reproducibility regardless of accommodation stress.

How might these results change the focus of research or clinical practice?

- This instrument is a clinically available and promising technology for in vivo lens assessments, potentially enhancing the understanding of the role of lens in the various ageing processes and disease pathophysiology.

INTRODUCTION

Non-invasive methods that enable in vivo visualisation of tissues are of particular relevance in ophthalmology because they provide important information about the physiology and diseases of the eye. Previous biometric research of human crystalline lenses includes an ex vivo study using specimens from autopsies,[1–3] and more recently, an in vivo human study with crystalline lens biometry using slit-lamp photography[4 5] and optical coherence tomography (OCT).[6] However, the accuracy of the optical techniques of Purkinje images[7] and Scheimpflug photography[8] is limited by the fact that the calculations of anterior lens surface curvature must be made through the optics of the anterior segment of the eye, while the posterior lens surface curvature measurement must be made through the lens itself,

which has an unknown refractive index gradient.[1] Moreover, the reproducibility of these methods is not fully understood. In recent years, OCT is increasingly used because it can provide anterior and posterior segment scans without contact with the eye, making the examination fast, safe and comfortable, and with a high axial and transverse spatial resolution. However, OCT imaging of the crystalline lens has imposed some challenges, including a limited axial range, compromised by the resolution of the spectrometer or a limited instantaneous linewidth of tuneable light source, which may be insufficient to image the entire anterior segment of the eye.[6] Thus, custom-made OCT has been used increasingly to study accommodation in vivo and in real time.[6 9–14]

The CASIA2 scanner (Tomey, Nagoya, Japan) is a novel commercial swept-source (SS) OCT, with a scan speed of 50 000 A-scans per second. With a frame size of 800 A-scans, it takes 0.016 s to capture a single cross-sectional image. This scanner improves optical coherence, producing a higher sensitivity for depth. The measurement range of the CASIA SS-1000 (Tomey), another new SS-OCT scanner specifically designed for anterior segment imaging, is φ16 mm×6 mm, but the CASIA2 can measure φ16 mm×13 mm. Therefore, it is possible to obtain data from the cornea to the posterior lens in one image.

While the CASIA2 enables automatic anterior and posterior curvature, and lens thickness measurements, due to deeper penetration in the axial direction compared with other commercially available OCT, its validity and reproducibility are still unknown. Therefore, the aim of this study was to investigate the intervisit and intraobserver variability of the CASIA2 OCT for in vivo crystalline lens biometric measurements.

MATERIALS AND METHODS

The Ethics Committee of Saitama Medical University approved this cross-sectional comparative study, which was conducted in accordance with the tenets of the Declaration of Helsinki. Subjects were included if they were at least 20 years old, fulfilled the eligibility requirements detailed below and signed an informed consent form between January 2016 and April 2016 at Saitama Medical University Hospital. All subjects underwent complete ocular examinations.

Subjects

Thirty healthy subjects with no history of ocular disease were consecutively invited for cataract and anterior chamber imaging in two separate visits within a week. Only one eye from each subject was randomly selected in the analysis. None of the subjects had apparent ocular disease, none had a history of intraocular surgery or laser procedure and none were using topical or systemic medication. Eyes with the best corrected visual acuity of <20/40, a spherical refraction of <−10.0 or >+3.0 dioptres (D) and a cylinder correction of >±3.0 D were excluded. Axial length data were obtained with OA-2000 (Tomey), and objective refraction was performed with the Tonoref 2 autorefractor/tonometer (Nidek Co., Aichi, Japan).

Anterior segment and lens imaging

The CASIA2 is a novel SS-OCT specifically designed for imaging the anterior segment. With a substantial improvement in scan speed (50 000 A-scans per second), it takes 0.016 s to capture a single cross-sectional image (each with 800 A-scans) 360°° around the anterior segment in 2.4 s. To avoid lid artefact, participants were instructed to pull down the lower lid against the lower orbital rim to expose the lower limbus, while the technician elevated the upper lid against the upper orbital rim to expose the upper limbus. None of the images obtained had any lid artefacts. After correcting refractive error by using a built-in program, the image was scanned at 0 dioptre (D) (static), −1 D, −3 D and −5 D accommodative stress.

Image analysis

The scans were adjusted for refraction distortion at the air corneal interface using the CASIA2 built-in program. The anterior and posterior lens curvatures and lens thickness were then measured by a single observer and calculated automatically by the CASIA2 scanner (figure 1).

Statistical analyses

Data are expressed as mean±SD for continuous variables. Baseline characteristics were compared using unpaired t-tests. In accordance with a previous ophthalmological study,[15 16] the intraobserver and intervisit reproducibility coefficient (RC) and intraclass correlation coefficient (ICC) were calculated. The RC was defined as $1.96\times\sqrt{2}\times$within-subject SD. The interpretation was that 95% of the difference between measurements obtained from two separate occasions would be less than the RC. ICC was classified as follows: <0.75 represented poor to moderate reliability, 0.75–0.90 represented good reliability and >0.90 represented excellent reliability for clinical measurements. We divided age into two categories: <35 years (n=17) and ≥35 years (n=13). A p value of <0.05 indicated a statistically significant difference. All statistical analyses were performed using JMP V.10.1 software (SAS Institute) and SPSS V.22 software (Japan IBM, Tokyo, Japan).

RESULTS

The mean (SD) age of the 30 subjects was 35.6 (11.7) years and the mean spherical error was −2.7 (2.8) D. The mean axial length was 24.8 (1.5) mm (table 1). Anterior lens curvature and lens thickness were

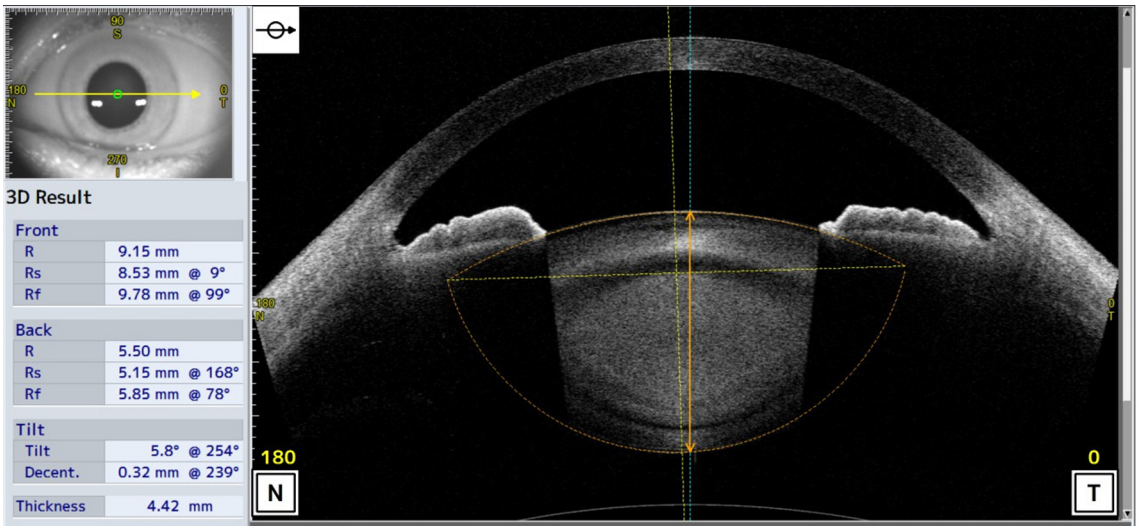

Figure 1 Optical coherence tomography images obtained from the CASIA2 anterior and posterior lens boundary are automatically drawn (orange dot lines), and their curvatures are calculated by the built-in software. Optic axis of lens (vertical orange dot lines) and vertex normal (vertical blue solid line) are automatically drawn and crystalline lens thickness is also calculated by the built-in software (vertical orange solid line).

Table 1 Baseline characteristics of the subjects

	Overall (n=30)	Younger (age<35) (n=17)	Older (age≥35) (n=13)	p Value*
Male, n (%)	9 (30)	5 (29)	4 (31)	
Age (years)	35.6±11.7	26.6±4.3	47.2±6.5	<0.001
Spherical equivalent error (D)	−2.7±2.8	−3.5±2.9	−2.7±2.8	0.070
Axial length (mm)	24.8±1.5	25.3±1.4	24.2±1.5	0.054
Corneal thickness (mm)	520.1±25.5	519.2±29.2	521.2±20.9	0.832
Crystalline lens biometry				
Static condition (±0 D)				
Anterior lens curvature (mm)	10.4±1.5	11.5±1.3	9.5±1.3	<0.001
Posterior lens curvature (mm)	5.8±0.4	6.1±0.4	5.8±0.3	0.056
Lens thickness (mm)	3.9±0.3	3.7±0.2	4.2±0.3	<0.001
−1 D accommodation stimuli				
Anterior lens curvature (mm)	9.5±1.3	11.3±1.3	10.3±1.6	<0.001
Posterior lens curvature (mm)	5.8±0.4	6.0±0.4	5.7±0.3	0.054
Lens thickness (mm)	3.9±0.3	3.7±0.2	4.2±0.3	<0.001
−3 D accommodation stimuli				
Anterior lens curvature (mm)	9.7±1.3	10.4±1.3	9.0±0.9	<0.001
Posterior lens curvature (mm)	5.8±0.4	5.9±0.4	5.7±0.4	0.072
Lens thickness (mm)	4.0±0.3	3.7±0.2	4.2±0.3	<0.001
−5 D accommodation stimuli				
Anterior lens curvature (mm)	8.9±0.9	8.9±0.9	8.9±0.9	0.127
Posterior lens curvature (mm)	5.6±0.3	5.6±0.3	5.6±0.3	0.490
Lens thickness (mm)	4.0±0.3	3.9±0.3	4.2±0.3	<0.001

Plus-minus values are means±SD.
*Unpaired t-test between younger age and older age.
D, dioptre.

Table 2 Intervisit/intraobserver RC and ICC of in vivo lens measurements

	RC (95% CI)		ICC (95% CI)	
	Intraobserver	Intervisit	Intraobserver	Intervisit
±0 D				
Anterior curvature (mm)	1.208 (0.728 to 1.688)	0.900 (0.550 to 1.249)	0.857 (0.724 to 0.929)	0.914 (0.828 to 0.958)
Posterior curvature (mm)	0.287 (0.178 to 0.396)	0.225 (0.150 to 0.299)	0.879 (0.763 to 0.940)	0.933 (0.864 to 0.968)
Lens thickness (mm)	0.076 (0.044 to 0.107)	0.062 (0.040 to 0.085)	0.987 (0.972 to 0.994)	0.992 (0.983 to 0.996)
−1 D accommodation stimuli				
Anterior curvature (mm)	1.254 (0.682 to 1.853)	0.911 (0.527 to 1.294)	0.832 (0.680 to 0.908)	0.898 (0.797 to 0.950)
Posterior curvature (mm)	0.276 (0.189 to 0.363)	0.230 (0.158 to 0.303)	0.898 (0.799 to 0.950)	0.929 (0.856 to 0.965)
Lens thickness (mm)	0.094 (0.055 to 0.133)	0.054 (0.035 to 0.073)	0.980 (0.958 to 0.990)	0.994 (0.988 to 0.997)
−3 D accommodation stimuli				
Anterior curvature (mm)	0.989 (0.627 to 1.351)	0.800 (0.513 to 1.087)	0.865 (0.734 to 0.934)	0.906 (0.809 to 0.955)
Posterior curvature (mm)	0.299 (0.178 to 0.419)	0.2221 (0.138 to 0.304)	0.832 (0.679 to 0.916)	0.921 (0.841 to 0.962)
Lens thickness (mm)	0.065 (0.043 to 0.087)	0.074 (0.051 to 0.098)	0.992 (0.983 to 0.996)	0.995 (0.989 to 0.997)
−5 D accommodation stimuli				
Anterior curvature (mm)	0.824 (0.541 to 1.108)	0.789 (0.486 to 1.092)	0.831 (0.677 to 0.915)	0.828 (0.662 to 0.916)
Posterior curvature (mm)	0.277 (0.182 to 0.372)	0.270 (0.172 to 0.368)	0.874 (0.754 to 0.938)	0.840 (0.692 to 0.921)
Lens thickness (mm)	0.072 (0.041 to 0.104)	0.132 (0.034 to 0.232)	0.984 (0.983 to 0.996)	0.942 (0.877 to 0.972)

D, dioptre; ICC, intraclass correlation coefficient; RC, reproducibility coefficient.

significantly different between age groups, and these differences decreased with increasing accommodative stimuli. Table 2 shows the intraobserver and intervisit RCs and ICC. The intraobserver and intervisit RCs ranged from 0.824 to 1.254 mm and 0.789 mm to 0.911 mm for anterior lens curvature, from 0.276 to 0.299 mm and 0.221 to 0.270 mm for posterior lens curvature, and from 0.065 to 0.094 mm and 0.054 to 0.132 mm for lens thickness, respectively. The intraobserver and intervisit ICCs ranged from 0.831 to 0.865 and 0.828 to 0.914 for anterior lens curvature, from 0.832 to 0.898 and 0.840 to 0.933 for posterior lens curvature and from 0.980 to 0.992 and 0.942 to 0.995 for lens thickness, respectively. High ICC values were observed for the measurements regardless of accommodative stimuli. The agreement between the values was analysed using Bland-Altman plots (figure 2). It is evident from figure 2 that there is no substantial bias between the measurements and that close agreement was found for the majority of subjects. The 95% limits of agreement among the measurements were +11.82% to −19.34% for anterior curvature, +4.97% to −7.60% for posterior curvature and +3.33% to −2.09% for lens thickness. There was no observable trend between per cent difference (bias) and mean measurement value. Table 3 shows the intraobserver and intervisit RCs according to age group. While the intraobserver and intervisit RCs were similar, RCs in younger subjects tended to be larger than those in older subjects.

DISCUSSION

The principal finding of this study is that the novel commercially available SS-OCT provides good

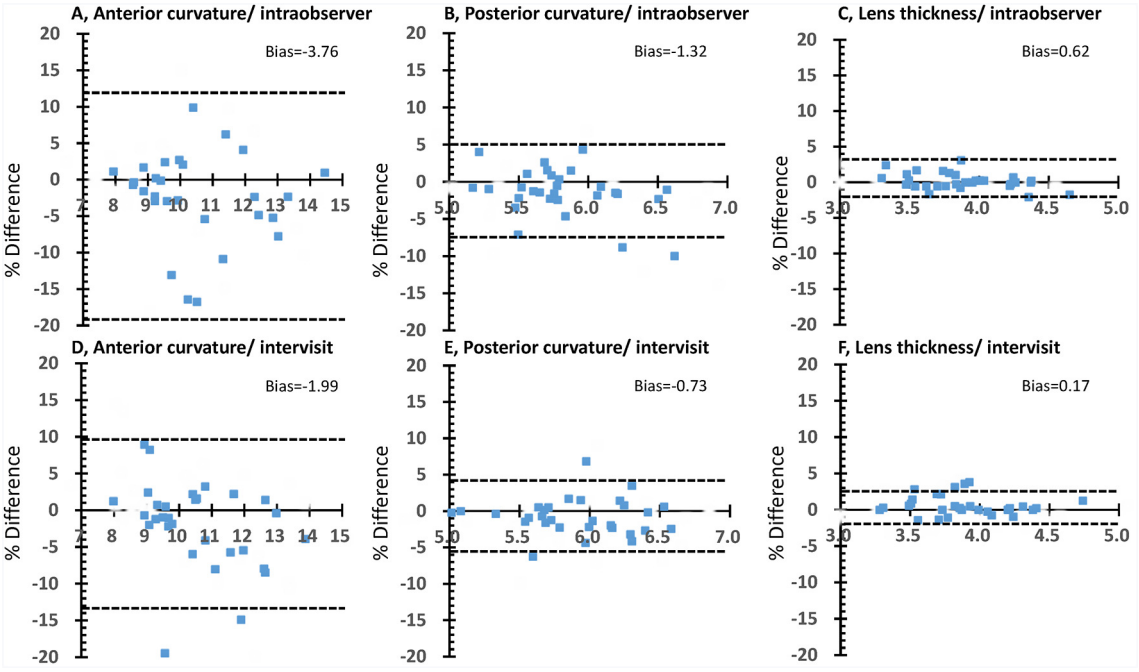

Figure 2 Bland-Altman plots for intraobserver and intervisit measurements at static condition (±0 D). A–C, Bland-Altman plots of intraobserver measurements. There is no substantial bias between these measurements. The 95% limits of agreement are +11.82% to −19.34% for anterior curvature (A), +4.97% to −7.60% for posterior curvature (B) and +3.33% to −2.09% for lens thickness (C). (D–F) Bland-Altman plots of intervisit measurements. There is no substantial bias between these measurements. The 95% limits of agreement are +9.57% to −13.55% for anterior curvature (D), +4.13% to −5.59% for posterior curvature (E) and +2.40% to −2.05% for lens thickness (F).

reproducible measurements of anterior and posterior lens curvatures and lens thickness. It can be useful for cataract assessments, measuring structural changes in accommodation, and for evaluating longitudinal changes in human lens biometry.

Recently, some custom-made OCTs have successfully imaged the whole crystalline lens in a single shot using multiple reference arms,[12–14] multiple light sources[17] and a vertical cavity surface-emitting laser device.[18] However, these instruments are laboratory based and have limited clinical application. In contrast to these devices, the CASIA2 is a commercially available OCT system and its built-in program enables the automatic calculation of entire in vivo crystalline lens images. To our knowledge, this is the first clinical report regarding the use of a CASIA2 scanner. An assessment of reproducibility is an essential tool for the evaluation of any imaging modality that is operator dependent and subject dependent. Hence, we calculated RCs and ICCs and found high reproducibility, regardless of accommodation, when measured across separate imaging sessions. Recent studies reported that the repeatability of ocular biometry measurements using SS-OCT was good or excellent.[15 19–21] Regarding the repeatability of SS-OCT for anterior segments, Neri *et al*[19] reported that the ICC of lens thickness measurements was 0.991, and Liu *et al*[15] reported an ICC of anterior chamber angle measurements of ≥0.83 with 30 healthy subjects. These values are comparable to those of the current study.

The strength of this device is its ability to calculate posterior lens curvature automatically. Accurate calculations of curvature require a high signal to noise ratio and minimal involuntary eye movement during fixation. The CASIA2 scanner is ideal for this purpose because it only needs 0.016 s to capture a single cross-sectional image. In the present study, no subjects had to be excluded because of insufficient image quality. Interestingly, the posterior lens curvature and lens thickness measurements tended to have better reproducibility than anterior curvature measurements (figure 2), even though the signal strength in OCT generally decreases with deeper penetration in the axial direction. This might be due to subject-related factors rather than device-related effects. Anterior curvature in younger subjects was significantly different from the older subjects, and was steeper with accommodative stimuli (table 1), while the RC in the static state in the younger group tended to be worse than that in the older age group (table 3). Thus, the relatively wide variability of anterior lens curvature may be due to accommodative changes such as accommodative microfluctuations.

Another strength of this novel SS-OCT scanner is that the light source of the central wavelength is an infrared light of 1310 nm, which is longer than that in other clinically available spectral-domain OCT

Table 3 Intervisit/intraobserver RC of in vivo lens measurements according to age categories

	Intraobserver (95% CI)		Intervisit (95% CI)	
	Younger (<35 years)	Older (≥35 years)	Younger (<35 years)	Older (≥35 years)
±0 D				
Anterior curvature (mm)	1.571 (0.957 to 2.185)	0.733 (0.031 to 1.435)	1.133 (0.681 to 1.586)	0.595 (0.078 to 1.112)
Posterior curvature (mm)	0.330 (0.117 to 0.469)	0.240 (0.072 to 0.406)	0.230 (0.129 to 0.331)	0.218 (0.103 to 0.333)
Lens thickness (mm)	0.094 (0.053 to 0.135)	0.052 (0.005 to 0.098)	0.077 (0.048 to 0.106)	0.043 (0.010 to 0.077)
−1 D accommodation stimuli				
Anterior curvature (mm)	1.706 (0.979 to 2.434)	0.662 (−0.064 to 1.388)	1.072 (0.562 to 1.583)	0.700 (0.116 to 1.284)
Posterior curvature (mm)	0.314 (0.210 to 0.418)	0.227 (0.065 to 0.388)	0.253 (0.156 to 0.350)	0.200 (0.090 to 0.312)
Lens thickness (mm)	0.124 (0.075 to 0.174)	0.055 (−0.007 to 0.116)	0.061 (0.036 to 0.086)	0.045 (0.016 to 0.074)
−3 D accommodation stimuli				
Anterior curvature (mm)	1.328 (0.893 to 1.763)	0.508 (−0.009 to 1.026)	1.045 (0.694 to 1.397)	0.453 (0.034 to 0.871)
Posterior curvature (mm)	0.434 (0.292 to 0.576)	0.121 (−0.041 to 0.284)	0.242 (0.130 to 0.354)	0.194 (0.066 to 0.322)
Lens thickness (mm)	0.083 (0.055 to 0.111)	0.042 (0.009 to 0.074)	0.081 (0.050 to 0.113)	0.065 (0.030 to 0.101)
−5 D accommodation stimuli				
Anterior curvature (mm)	0.950 (0.547 to 1.353)	0.660 (0221 to 1.098)	1.008 (0.622 to 1.394)	0.497 (0.051 to 0.943)
Posterior curvature (mm)	0.334 (0.210 to 0.458)	0.202 (0.060 to 0.345)	0.262 (0.130 to 0.395)	0.280 (0.129 to 0.431)
Lens thickness (mm)	0.079 (0.036 to 0.122)	0.064 (0.013 to 0.115)	0.149 (0.016 to 0.283)	0.011 (0.000 to 0.024)

D, dioptre; RC, reproducibility coefficient.

scanners, and the effects of the measurement light on pupil movement and miosis are minimal. While slit-lamp observations comprise another in vivo method for the evaluation of lens biometry, it is difficult to use these for the evaluation of anterior and posterior lens curvatures without mydriasis. Therefore, the effect of detailed accommodative change on the lens structure cannot be analysed due to mydriasis. However, this novel SS-OCT imaging technique can reveal the effect of lens structure change on accommodation.

A major limitation of this study is that all included volunteers were healthy and relatively young, and demonstrated clear lens visibility. Repeatability and reproducibility would be expected to decrease in eyes with a less distinct boundary on OCT images.

CONCLUSION

This study demonstrated that this novel SS-OCT, involving deeper penetration in the axial direction and a built-in program, can provide reproducible measurements of human crystalline lens biometry. This instrument is a promising technology for in vivo lens assessments, potentially enhancing the understanding of the role of lens in the various ageing processes and disease pathophysiology.

Acknowledgement The authors wish to thank Miss Kobori and Kumagai for help in preparing the study and clinical input.

Contributors TS, NK and SI conceived and designed the experiments. TS, NK, SI and HI collected the samples and performed the experiments. TS, HI and

NK analysed the data. TS and HI wrote the manuscript and NK, NY, IK and KS reviewed the manuscript.

Funding This study was supported in part by Takeda Science Foundation, Tokyo, Japan; Grant-in-Aid for Young Researchers from Saitam Medical University Hospital and Japan Society for the Promotion of Science KAKENHI grant no 15K21335.

Competing interests TS: Alcon (travel grant). NK, SI, HI, NY, IK, KS: none.

Provenance and peer review Not commissioned; externally peer reviewed.

REFERENCES

1. Glasser A, Campbell MC. Biometric, optical and physical changes in the isolated human crystalline lens with age in relation to presbyopia. *Vision Res* 1999;39:1991–2015.
2. Sun M, Birkenfeld J, de Castro A, *et al*. OCT 3-D surface topography of isolated human crystalline lenses. *Biomed Opt Express* 2014;5:3547–61.
3. Rosen AM, Denham DB, Fernandez V, *et al*. In vitro dimensions and curvatures of human lenses. *Vision Res* 2006;46:1002–9.
4. Brown N. The change in lens curvature with age. *Exp Eye Res* 1974;19:175–83.
5. Dubbelman M, Van der Heijde GL. The shape of the aging human lens: curvature, equivalent refractive index and the lens paradox. *Vision Res* 2001;41:1867–77.
6. Gambra E, Ortiz S, Perez-Merino P, *et al*. Static and dynamic crystalline lens accommodation evaluated using quantitative 3-D OCT. *Biomed Opt Express* 2013;4:1595–609.
7. Rosales P, Marcos S. Phakometry and lens tilt and decentration using a custom-developed Purkinje imaging apparatus: validation and measurements. *J Opt Soc Am A Opt Image Sci Vis* 2006;23:509–20.
8. Dubbelman M, Van der Heijde GL, Weeber HA, *et al*. Changes in the internal structure of the human crystalline lens with age and accommodation. *Vision Res* 2003;43:2363–75.
9. Pérez-Merino P, Velasco-Ocana M, Martinez-Enriquez E, *et al*. OCT-based crystalline lens topography in accommodating eyes. *Biomed Opt Express* 2015;6:5039–54.
10. Özyol P, Özyol E. Agreement between swept-source optical biometry and Scheimpflug-based topography measurements of anterior segment parameters. *Am J Ophthalmol* 2016;169:73–8.
11. Martinez-Enriquez E, Sun M, Velasco-Ocana M, *et al*. Optical coherence tomography based estimates of crystalline lens volume, equatorial diameter, and plane position. *Invest Ophthalmol Vis Sci* 2016;57:OCT600–10.
12. Zhong J, Tao A, Xu Z, *et al*. Whole eye axial biometry during accommodation using ultra-long scan depth optical coherence tomography. *Am J Ophthalmol* 2014;157:1064–9.
13. Ruggeri M, Uhlhorn SR, De Freitas C, *et al*. Imaging and full-length biometry of the eye during accommodation using spectral domain OCT with an optical switch. *Biomed Opt Express* 2012;3:1506–20.
14. Tao A, Shao Y, Zhong J, *et al*. Versatile optical coherence tomography for imaging the human eye. *Biomed Opt Express* 2013;4:1031–44.
15. Liu S, Yu M, Ye C, *et al*. Anterior chamber angle imaging with swept-source optical coherence tomography: an investigation on variability of angle measurement. *Invest Ophthalmol Vis Sci* 2011;52:8598–603.
16. Li H, Leung CK, Cheung CY, *et al*. Repeatability and reproducibility of anterior chamber angle measurement with anterior segment optical coherence tomography. *Br J Ophthalmol* 2007;91:1490–2.
17. Dai C, Zhou C, Fan S, *et al*. Optical coherence tomography for whole eye segment imaging. *Opt Express* 2012;20:6109–15.
18. Grulkowski I, Liu JJ, Zhang JY, *et al*. Reproducibility of a long-range swept-source optical coherence tomography ocular biometry system and comparison with clinical biometers. *Ophthalmology* 2013;120:2184–90.
19. Neri A, Ruggeri M, Protti A, *et al*. Dynamic imaging of accommodation by swept-source anterior segment optical coherence tomography. *J Cataract Refract Surg* 2015;41:501–10.
20. Lee SY, Bae HW, Kwon HJ, *et al*. Repeatability and agreement of swept source and spectral domain optical coherence tomography evaluations of thickness sectors in normal eyes. *J Glaucoma* 2016;26:e46–e53.
21. Arriola-Villalobos P, Fernández-Vigo JI, Díaz-Valle D, *et al*. Lower tear meniscus measurements using a new anterior segment swept-source optical coherence tomography and agreement with Fourier-Domain optical coherence tomography. *Cornea* 2017;36:183–8.